

# Pacritinib Inhibition of IRAK1 Blocks Aberrant TLR8 Signalling by SARS-CoV-2 and HIV-1-Derived RNA

Grant R. Campbell<sup>a</sup> Pratima Rawat<sup>a</sup> Stephen A. Spector<sup>a, b</sup>

<sup>a</sup>Division of Infectious Diseases, Department of Pediatrics, University of California San Diego, La Jolla, CA, USA;

<sup>b</sup>Rady Children's Hospital, San Diego, CA, USA

## Keywords

SARS-CoV-2 · HIV-1 · TLR8 · Pacritinib · IRAK1

## Abstract

Macrophages promote an early host response to infection by releasing pro-inflammatory cytokines such as interleukin (IL) 1 $\beta$  (IL-1 $\beta$ ), tumour necrosis factor (TNF), and IL-6. One of the mechanisms through which cells sense pathogenic microorganisms is through Toll-like receptors (TLRs). IL-1 receptor-associated kinase (IRAK) 1, IRAK2, IRAK3, and IRAK4 are integral to TLR and IL-1 receptor signalling pathways. Recent studies suggest a role for aberrant TLR8 and NLRP3 inflammasome activation during both COVID-19 and HIV-1 infection. Here, we show that pacritinib inhibits the TLR8-dependent pro-inflammatory cytokine response elicited by GU-rich single-stranded RNA derived from SARS-CoV-2 and HIV-1. Using genetic and pharmacologic inhibition, we demonstrate that pacritinib inhibits IRAK1 phosphorylation and ubiquitination which then inhibits the recruitment of the TAK1 complex to IRAK1, thus inhibiting the activation of downstream signalling and the production of pro-inflammatory cytokines.

© 2022 The Author(s).

Published by S. Karger AG, Basel

## Introduction

Severe acute respiratory syndrome coronavirus 2 (SARS-CoV-2) is the aetiologic agent of COVID-19. Most adults and children infected with SARS-CoV-2 are either asymptomatic or experience mild symptoms. However, a subset of infections progress to severe disease and cytokine release syndrome (CRS, also called cytokine storm) characterised by alterations in the myeloid-cell compartment [1, 2], impaired interferon (IFN) response [3–5] and T cell function [6–9], the production of autoantibodies [10], and the uncontrolled release and high circulating levels of pro-inflammatory cytokines including interleukin (IL) 1 $\beta$  (IL-1 $\beta$ ), IL-6, and tumour necrosis factor (TNF) [5, 11–13]. The presence of CRS is often associated with increased viral load and extensive immune-mediated lung injury leading to acute respiratory distress syndrome, multi-organ failure, and death [14–18]. Human immunodeficiency virus type 1 (HIV-1) pathogenesis is also associated with immune activation and chronic inflammation despite effective viral suppression from anti-retroviral treatment (ART) [19], which contributes to non-AIDS-related inflammatory diseases in persons living with HIV-1 (PLWH) [20].

Pratima Rawat's current address: Microbiologics Inc., San Diego, CA, USA.

Toll-like receptors (TLR) are pattern recognition receptors that recognise specific pathogen-associated molecular patterns and are critical in regulating innate immune responses and in inducing and directing adaptive immunity. Four TLR family members recognise nucleic acid PAMPs with TLR7 and TLR8 recognising guanine/uridine-rich single-stranded RNA (GU-rich ssRNA) degradation products [21]. The IL-1 receptor-associated kinases (IRAK) IRAK1, IRAK2, IRAK3, and IRAK4 are key mediators of TLR signalling, all possess a central kinase domain, and all are classified as serine/threonine kinases; however, only IRAK1 and IRAK4 possess demonstrable kinase activity [22]. Human TLR8 exists as a homodimer within the endosomes of macrophages, monocytes, and myeloid dendritic cells [23, 24]. Upon endosomal or autophagosomal engulfment, the fragmentation of viral RNA by the lysosomal endoribonuclease RNase T2 generates multiple GU-rich ssRNA fragments that are detectable by TLR8 [21, 25–27]. These RNA fragments bind TLR8 cooperatively at two distinct sites in the N-terminal domain, inducing a conformational change of the TLR8 dimer, resulting in the recruitment of the adaptor protein MYD88. MYD88 then recruits IRAK4 through N-terminal death domain interactions that induce the dimerisation and *trans*-autophosphorylation of IRAK4 to form the oligomeric myddosome [28–30]. This myddosome then recruits IRAK1, IRAK2, and/or IRAK3 [31, 32]. The recruitment of IRAK1 results in its activation, possibly through IRAK4-induced dimerisation mediated through an allosteric mechanism, although this has yet to be fully elucidated [30–33]. Activated IRAK1 then phosphorylates and activates pellino E3 ubiquitin protein ligase (PELI) 1 and PELI2 and is itself extensively phosphorylated by IRAK4, allowing the recruitment of the E3 ubiquitin ligase TNF receptor-associated factor 6 (TRAF6) to the myddosome. The IRAK1-TRAF6 interaction activates TRAF6, which in combination with PELI1, PELI2, and UBE2N-UBE2V1, leads to the lysine 63-ubiquitination (K63Ub) of IRAK1 [34, 35]. TRAF6 also recruits LUBAC where it interacts with the K63Ub-IRAK1 to attach covalently Met1-linked ubiquitin oligomers (M1Ub) to K63Ub on IRAK1 forming K63/M1 ubiquitin hybrids [36]. Notably, IRAK1 activation requires neither phosphorylation nor ubiquitination [30, 36]. The IRAK1-TRAF6 complex is then released from the myddosome where the K63/M1-Ub hybrids recruit and activate the TAK1 and IKK complexes, leading to downstream activation of numerous pro-inflammatory mediators, including MAP kinases and NF- $\kappa$ B, that results in the ex-

pression of pro-inflammatory cytokines including IL-6, IL-12, IL-27, TNF, IFN $\gamma$ , and IL-1 $\beta$  [37–39].

As IRAKs are critical for TLR8 signalling and play direct roles in the TLR-mediated activation of the NLRP3 inflammasome and the subsequent generation of IL-1 $\beta$  and other important pro-inflammatory cytokines [40], inhibiting IRAKs has potential therapeutic benefits [22, 41–43]. Pacritinib is a small-molecule, ATP-competitive, macrocyclic inhibitor of JAK2/FMS-like tyrosine kinase 3 [44] which also shows moderate selectivity against IRAK1 versus IRAK4 (IC<sub>50</sub>: 6 nM and 177 nM, respectively) [43]. Here, we provide evidence that pacritinib effectively inhibits the TLR8-mediated pro-inflammatory cytokine response to GU-rich ssRNAs from SARS-CoV-2 and HIV-1 at clinically relevant concentrations.

## Materials and Methods

### Primary Human Cells

Peripheral blood mononuclear cells were isolated from whole blood by density-gradient centrifugation over Ficoll-Paque Plus (GE Healthcare). Monocyte-derived macrophages were prepared from peripheral blood mononuclear cells by adherence as previously described [45].

### Chemicals

RNA649 (5'-GUCAGAGUGUGUACUUG-3'; position 24649–24665 nt in the SARS-CoV-2 genome [S2 spike protein region] [accession number: NC\_045512.2]) [26], RNA649A (a derivative of RNA649 in which adenosine replaces all uracil nucleotides), RNA40 (5'-GCCCGUCUGUUGUGUGACUC-3'; at U5 region 108–127 nt of the HIV-1 genome [accession number: NC\_001802.1]) [21], and RNA41 (a derivative of RNA40 in which adenosine replaces all uracil nucleotides) were synthesised by Integrated DNA Technologies. LyoVec (InvivoGen), a cationic lipid-based transfection reagent, was used to complex GU-rich ssRNA in a 2:1 (LyoVec:RNA) ratio as previously described [26]. Pacritinib (also known as SB1518) and zimlovisertib were obtained from Selleck Chemicals. Lambda protein phosphatase and MG132 were purchased from Sigma-Aldrich. Recombinant human ubiquitin-specific peptidase 2 was purchased from R&D Systems. Corresponding volumes of each vehicle were used in controls: endotoxin-free water for GU-rich ssRNA, RNA controls, and LyoVec (InvivoGen); DMSO (Sigma-Aldrich) for pacritinib, zimlovisertib, and MG132; lambda protein phosphatase buffer (Sigma-Aldrich) for lambda protein phosphatase; and 50 mM HEPES pH 8, 150 mM NaCl, 0.1 mM EDTA, and 1 mM DTT (all Sigma-Aldrich) for recombinant human ubiquitin specific peptidase 2.

### Enzyme-Linked Immunosorbent Assay

IL-1 $\beta$  (Cat# DLB50 and DY201), IL-6 (Cat# DY206), and TNF (Cat# DY207) were measured in cell culture supernatants using enzyme-linked immunosorbent assay kits obtained from R&D Systems according to the manufacturer's instructions.

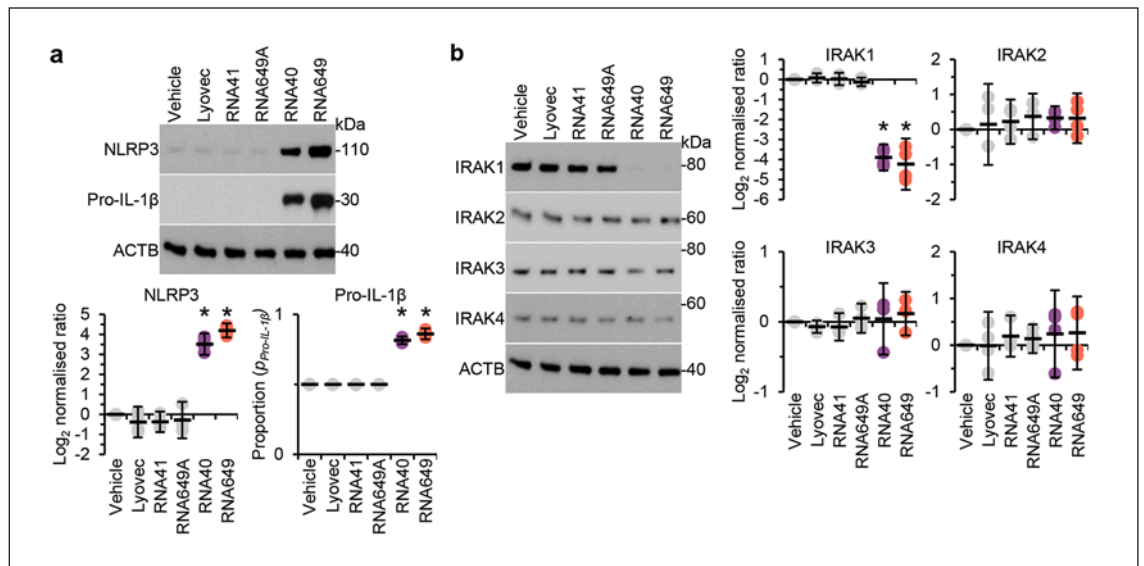


**Fig. 1.** GU-rich ssRNAs induce the disappearance of IRAK1. Macrophages were treated for 24 h with 5  $\mu\text{g mL}^{-1}$  GU-rich ssRNA or controls. **a** *Top*, representative western blots of pro-IL-1 $\beta$ , NLRP3, and ACTB. *Bottom*, densitometric analysis of blots.  $N = 4$ . **b** *Left*, representative western blots of IRAK1, IRAK2, IRAK3, IRAK4, and ACTB. *Right*, densitometric analysis of blots.  $N = 4$ .

#### siRNA Transfection

Macrophages were transfected with Ambion Silencer Select *TLR8* (ID# s27920), *P2XR7* (ID# s9959), or control (Cat# 4390846) siRNA (siNS) using lipofectamine RNAiMAX transfection reagent (Invitrogen) in Opti-MEM (Gibco) according to the manufacturer's instructions. Forty-eight hours later, cells were analysed for target gene silencing and used in experiments. Transfection efficiency was assessed using BLOCK-iT Alexa Fluor Red Fluorescent Control (Invitrogen) on a BD FACSCalibur flow cytometer [46].

#### Western Blotting

Cell lysis, co-immunoprecipitation, and western blotting were performed as previously described [46, 47]. Briefly, cell lysates were prepared using 20 mM HEPES, 150 mM NaCl, and 1 mM EDTA supplemented with 1% (vol/vol) Triton X-100 and 1% (vol/vol) Thermo Scientific Halt protease and phosphatase inhibitor cocktail. Co-immunoprecipitation was performed using the Pierce Co-Immunoprecipitation Kit with 50  $\mu\text{g}$  anti-IRAK1 (Cat# ab180747, RRID:AB\_2895218) from Cell Signaling and 50  $\mu\text{g}$  cell lysates according to the manufacturer's directions. Incubation of immunoprecipitates with phosphatases and deubiquitinases was performed exactly as previously described [30]. Cell lysates and immunoprecipitates were resolved using 2-(bis[2-hydroxyethyl]amino)-2-(hydroxymethyl) propane-1,3-diol-buffered (wt/vol) polyacrylamide gels, transferred to 0.2- $\mu\text{m}$  polyvinylidene difluoride membranes, probed with primary antibodies overnight at 4°C, followed by detection using alkaline phosphatase-tagged secondary antibodies (Invitrogen) and 0.25 mM CDP-Star supplemented with 5% (vol/vol) Nitro-Block II (both Applied Biosystems). The primary antibodies raised against the following were used in western blots: ERK1/2 (Cat# 4695, RRID:AB\_390779), phospho-ERK1/2 (Thr202/Tyr204) (Cat# 4370, RRID:AB\_2315112), I $\kappa$ B $\alpha$  (Cat# 4812, RRID:AB\_10694416), phospho-I $\kappa$ B $\alpha$  (Ser<sup>32</sup>) (Cat#

2859, RRID:AB\_561111), IL-1 $\beta$  (Cat# 12703, RRID:AB\_2737350), IRAK1 (Cat# 4504, RRID:AB\_1904032), IRAK2 (Cat# 4367, RRID:AB\_2126268), IRAK3 (Cat# 4369, RRID:AB\_2264868), IRAK4 (Cat# 4363, RRID:AB\_2126429), IRF5 (Cat# 20261, RRID:AB\_2798838), JNK (Cat# 9252, RRID:AB\_2250373), phospho-JNK (Thr<sup>183</sup>/Tyr<sup>185</sup>) (Cat# 4671, RRID:AB\_331338), NLRP3 (Cat# 13,158, RRID:AB\_2798134), P2XR7 (Cat# 13809, RRID:AB\_2798319), p38 MAPK (Cat# 9212, RRID:AB\_330713), phospho-p38 MAPK (Thr<sup>180</sup>/Tyr<sup>182</sup>) (Cat# 4511, RRID:AB\_2139682), TAB2 (Cat# 3745, RRID:AB\_2297368), TAK1 (Cat# 5206, RRID:AB\_10694079), and TRAF6 (Cat# 67591, RRID:AB\_2904212) from Cell Signaling Technology, ACTB (Cat# A2228, RRID:AB\_476697) from Sigma-Aldrich, phospho-IRAK1 (Thr<sup>209</sup>) (Cat# PA5-38633, RRID:AB\_2555228) from Invitrogen, and *TLR8* (Cat# NBP2-24917, RRID:AB\_2847894) from Novus Biologicals. Phospho-IRF5 (Ser<sup>462</sup>) was obtained from the MRC Protein Phosphorylation and Ubiquitylation Unit at the University of Dundee, Scotland (Cat# IRF5 S509D, RRID:AB\_2905520). Relative densities of the target bands were compared to the reference (ACTB) and were calculated using Fiji from the Max Planck Institute of Molecular Cell Biology and Genetics (Fiji, RRID:SCR\_002285) [48].

#### Lactose Dehydrogenase Assay

Lactate dehydrogenase release from cells was measured using a mixture of diaphorase/NAD<sup>+</sup> and 3-(4-iodophenyl)-2-(4-nitrophenyl)-5-phenyl-2H-tetrazol-3-ium chloride/sodium 2-hydroxypropanoate and per cent cytotoxicity calculated according to the manufacturer's protocol (Roche).

#### Flow Cytometry

A total of  $1 \times 10^5$  macrophages were harvested and stained with Alexa Fluor 488-conjugated annexin V (Cat# A13201; Invitrogen) and 1  $\mu\text{g/mL}$  propidium iodide (Cat# P3566; Invitrogen) in 10 mM

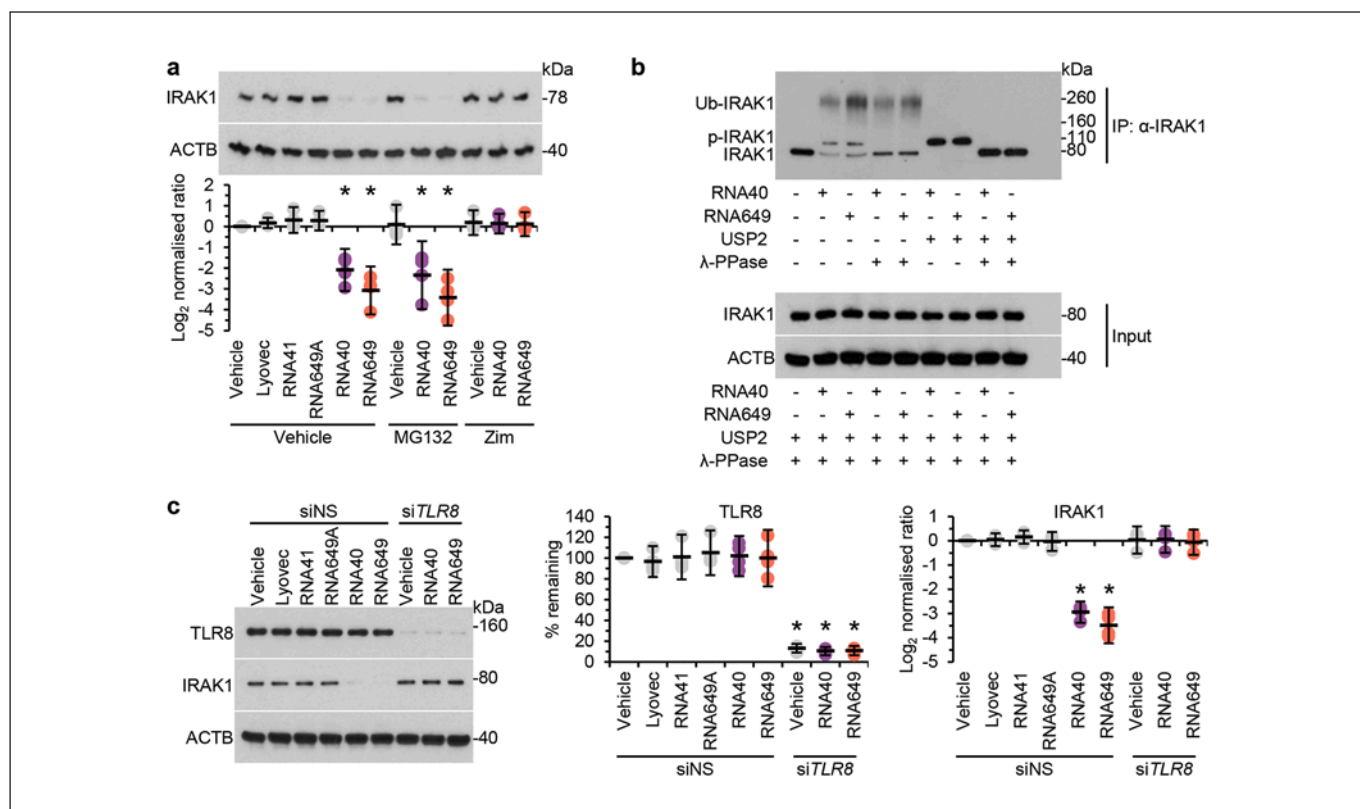


**Fig. 2.** GU-rich ssRNAs induce the phosphorylation and ubiquitination of IRAK1 through TLR8. **a** Macrophages were pretreated with 5  $\mu$ M MG132, 100 nM zimlovisertib (Zim), or vehicle control (vehicle) for 2 h, then treated for 24 h with 5  $\mu$ g mL<sup>-1</sup> GU-rich ssRNA or controls. *Top*, representative western blot of IRAK1 and ACTB. *Bottom*, densitometric analysis of blots.  $N = 4$ . **b** Macrophages were stimulated for 5 h with 5  $\mu$ g mL<sup>-1</sup> RNA40 or RNA649 and IRAK1 immunoprecipitated (IP) from the cell extracts; 30  $\mu$ L immunoprecipitated IRAK1 was incubated with or without 50 U

lambda protein phosphatase ( $\lambda$ -PPase) and/or 1.15  $\mu$ g recombinant human ubiquitin-specific peptidase 2 (USP2) and subjected to SDS/PAGE and western blotting with anti-IRAK1. Phosphorylated IRAK1 and phosphorylated and ubiquitinated IRAK1 are denoted by p-IRAK1 and Ub-IRAK1, respectively. **c** Macrophages were transfected with *TLR8* (siTLR8) or scrambled siRNA (siNS) for 48 h then treated with 5  $\mu$ g mL<sup>-1</sup> GU-rich ssRNA or controls for 24 h. *Left*, representative western blots of TLR8, IRAK1, and ACTB. *Right*, densitometric analysis of blots.  $N = 4$ .

HEPES, 140 mM NaCl, 2.5 mM CaCl<sub>2</sub>, pH 7.4, staining for 15 min at 4°C. Samples were then diluted 1:4 in 10 mM HEPES, 140 mM NaCl, 2.5 mM CaCl<sub>2</sub>, pH 7.4, before blinded acquisition using a BD FACSCalibur flow cytometer (BD Biosciences) using the 488-nm blue laser for excitation and 530/30 BP filter for detection of Alexa Fluor 488 emission and 670/LP filter for propidium iodide. Analysis was performed using FlowJo v. 10.8 software.

#### Statistics

Samples were assigned to experimental groups through simple random sampling. Sample size ( $n$ ) was determined using a 2-sample 2-sided equality test with power  $(1-\beta) = 0.8$ ,  $\alpha = 0.05$  and preliminary data where the minimum difference in outcome was at least 70%. Data are represented as dot blots with arithmetic means  $\pm$  95% confidence interval. Data were assessed for symmetry or skewness, using Pearson's skewness coefficient. Normalised ratiometric data were log<sub>2</sub>-transformed. When protein expression in the reference sample was zero, we used proportion statistics to analyse differences [46, 49]. Comparisons between

groups were performed using paired, two-tailed, Student's  $t$  test. In all experiments, differences were considered significant when  $p < 0.05$  ( $*p < 0.05$ ).

## Results

### GU-Rich ssRNA RNA649 and RNA40 Induce the TLR8-Mediated Phosphorylation and Ubiquitination of IRAK1

We previously identified a GU-rich ssRNA sequence from the spike protein of SARS-CoV-2 (RNA649) [26] and together with the previously described HIV-1-derived RNA40 [21] demonstrated that these GU-rich ssRNA elicit a TLR8-dependent pro-inflammatory cytokine response from primary human macrophages in the

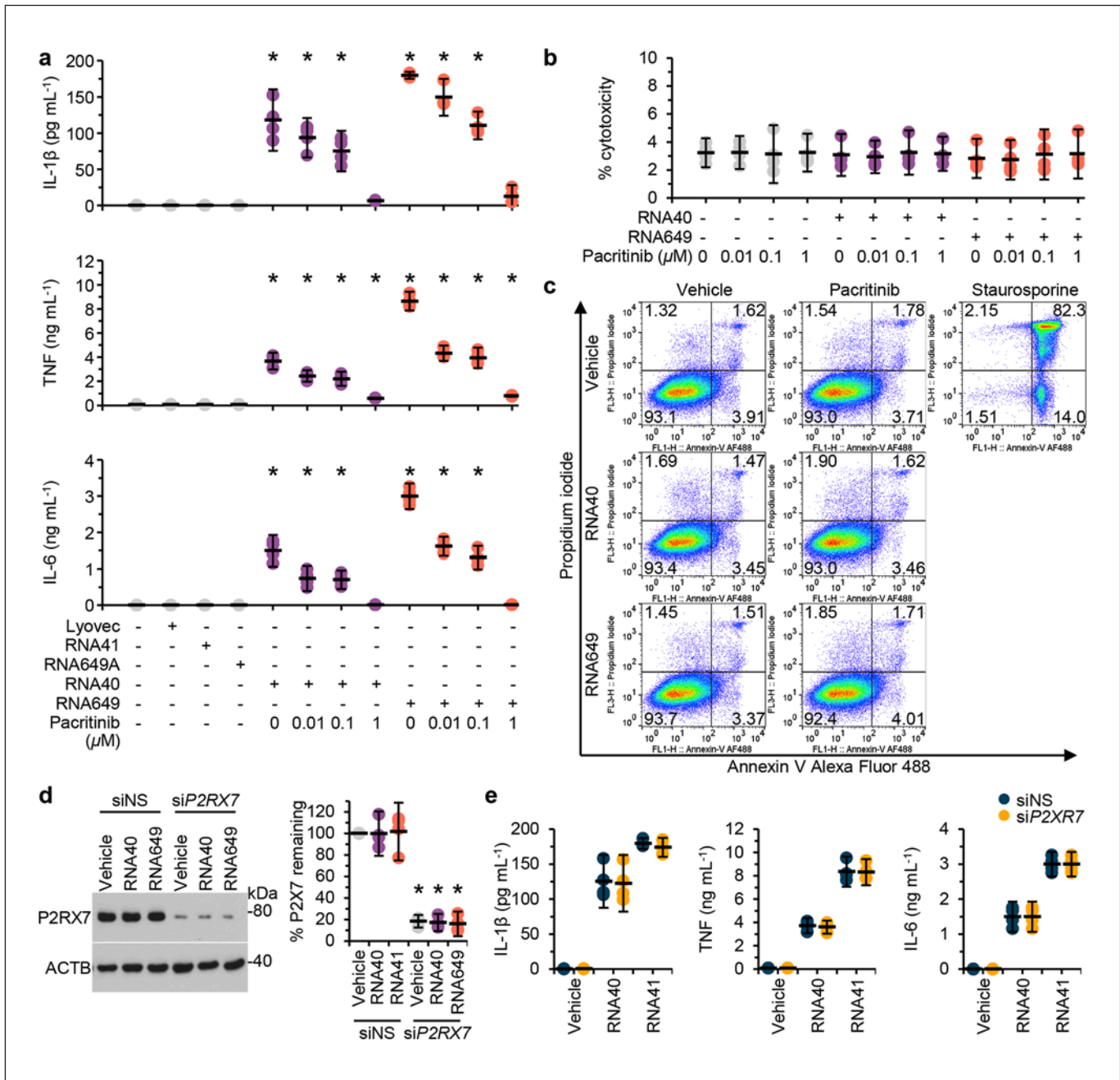


**Fig. 3.** Pacritinib inhibits GU-rich ssRNA induced pro-inflammatory cytokine secretion from macrophages. Macrophages (**a–c**) were pretreated with pacritinib or controls for 2 h and then treated for 24 h with 5  $\mu\text{g mL}^{-1}$  GU-rich ssRNA. *n* = 4. **a** Cell supernatants were collected and analysed for cytokines. **b** Aliquots of supernatants were spectrophotometrically tested for lactate dehydrogenase release, and per cent cytotoxicity was calculated. **c** Cells were harvested, stained with annexin V Alexa Fluor 488 and propidium

iodide, and then analysed using flow cytometry. 2  $\mu\text{M}$  staurosporine was added for 24 h as a positive control. Representative pseudocolour plots are shown. **d** Macrophages were transfected with *P2XR7* (siP2XR7) or scrambled siRNA (siNS) for 48 h and then treated with 5  $\mu\text{g mL}^{-1}$  GU-rich ssRNA or control for 24 h. *Left*, representative western blots of P2XR7 and ACTB. *Right*, densitometric analysis of blots. **e** Cell supernatants from (**d**) were collected and analysed for cytokines.

absence of pyroptosis [26]. Here, we examine whether the GU-rich ssRNA triggering and activation of the TLR8-signalling pathway involves IRAK1. Although it was thought that IRAK1 is proteasomally degraded after activation of TLR/IL-1R/MYD88-signalling as it becomes undetectable in western blots [50], it is now known that the rapid phosphorylation and ubiquitination of IRAK1 results in this loss of IRAK1 detection [30, 51, 52]. Both RNA649 and RNA40 induced the expression of pro-IL-1 $\beta$  and increased the expression of NLRP3 (shown in Fig. 1a) while also inducing the disappearance of IRAK1 (shown in Fig. 1b). The levels of IRAK2, IRAK3, and IRAK4 did not change (shown in Fig. 1b). Importantly, treatment with MG132, a cell-permeable proteasome and calpain inhibitor, failed to reverse the disappearance of IRAK1 from the blots (shown in Fig. 2a), indicating that IRAK1 was not degraded through the proteasome. To confirm that IRAK1 was indeed phosphorylated and/or ubiquitinated, we performed an IP for IRAK1 then treated the immunoprecipitates with a phosphatase and/or a deubiquitinase. We observed that both RNA649 and RNA40 induced the phosphorylation and ubiquitination of IRAK1, and we fully recovered the unmodified form of IRAK1 using a phosphatase with a deubiquitinase (shown in Fig. 2b). To confirm the role for TLR8 in the disappearance of IRAK1, we silenced *TLR8* and observed that *TLR8* silencing abolished the disappearance of IRAK1 from western blots (shown in Fig. 2c). Finally, we assessed whether the phosphorylation and ubiquitination of IRAK1 was dependent upon IRAK4. Treatment with the specific IRAK4 inhibitor zimlovisertib also restored the disappearance of IRAK1 from western blots, indicating that the phosphorylation and ubiquitination of IRAK1 by TLR8 triggering is dependent upon IRAK4 (shown in Fig. 2a).

#### *Pacritinib Inhibits TLR8-Mediated Cytokine Production*

We next examined whether inhibition of IRAK1 using pacritinib inhibits TLR8 signalling and the downstream generation of IL-1 $\beta$  and other important pro-inflammatory cytokines. Pacritinib dose-dependently inhibited both RNA649 and RNA40-induced IL-1 $\beta$ , TNF, and IL-6 secretion (shown in Fig. 3a), indicating that the inhibition of IRAK1 suppresses the endosomal TLR8 pro-inflammatory signalling pathways. Importantly, pacritinib had no discernible cytotoxic effect on human macrophages either alone or in the presence of the TLR8 agonists at all concentrations tested (shown in Fig. 3b, c). As pacritinib also inhibits JAK2 [44] and the purinergic receptor P2X

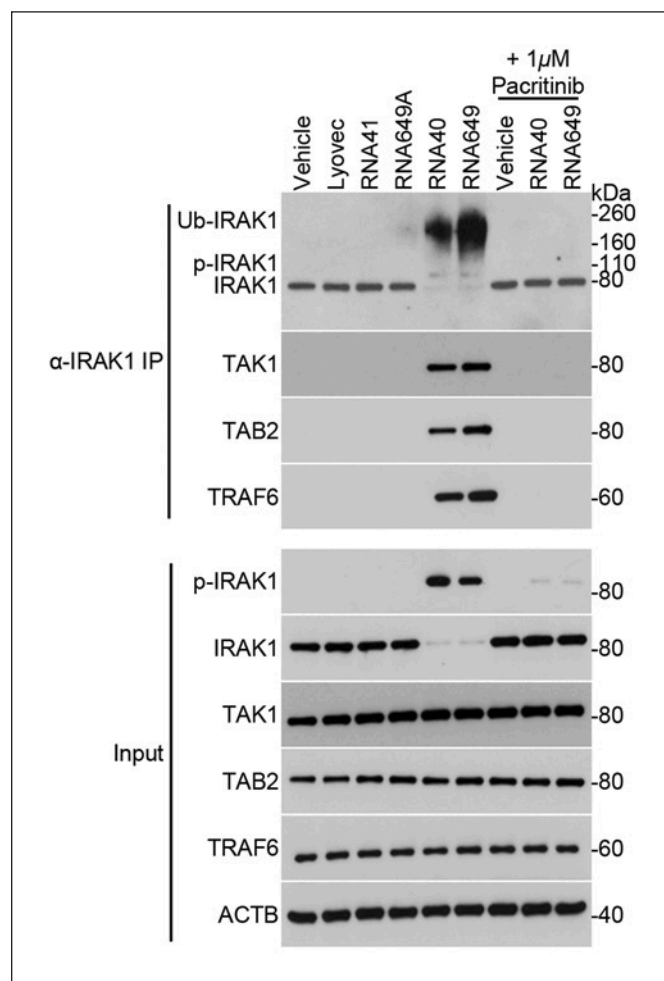


**Fig. 4.** Pacritinib inhibits the association of IRAK1 with TAK1. Macrophages were pretreated with pacritinib or controls for 2 h and then treated for 6 h with 5  $\mu\text{g mL}^{-1}$  GU-rich ssRNA.  $n = 4$ . Cells were lysed, and IRAK1 was immunoprecipitated (IP). The presence of phosphorylated, ubiquitinated, and total IRAK1, TAK1, TAB2, TRAF6, and ACTB was assayed by western blot.  $N = 4$ .

ligand gated ion channel 7 (P2RX7) which is involved in ATP-induced IL-1 $\beta$  secretion in primary human monocytes [53] shares a consensus sequence with JAK2 [54], we investigated whether P2RX7 was involved in the GU-rich ssRNA-mediated pro-inflammatory response using RNAi for *P2RX7* (shown in Fig. 3d). *P2RX7* silencing had no inhibitory effect on GU-rich ssRNA-mediated pro-inflammatory response (shown in Fig. 3e) confirming that P2RX7 is not involved in TLR-mediated inflammasome activation in human myeloid cells, in agreement with Gaidt et al. [53]. Thus, the pacritinib inhibition of the GU-rich ssRNA-mediated pro-inflammatory response is not through P2RX7 inhibition.

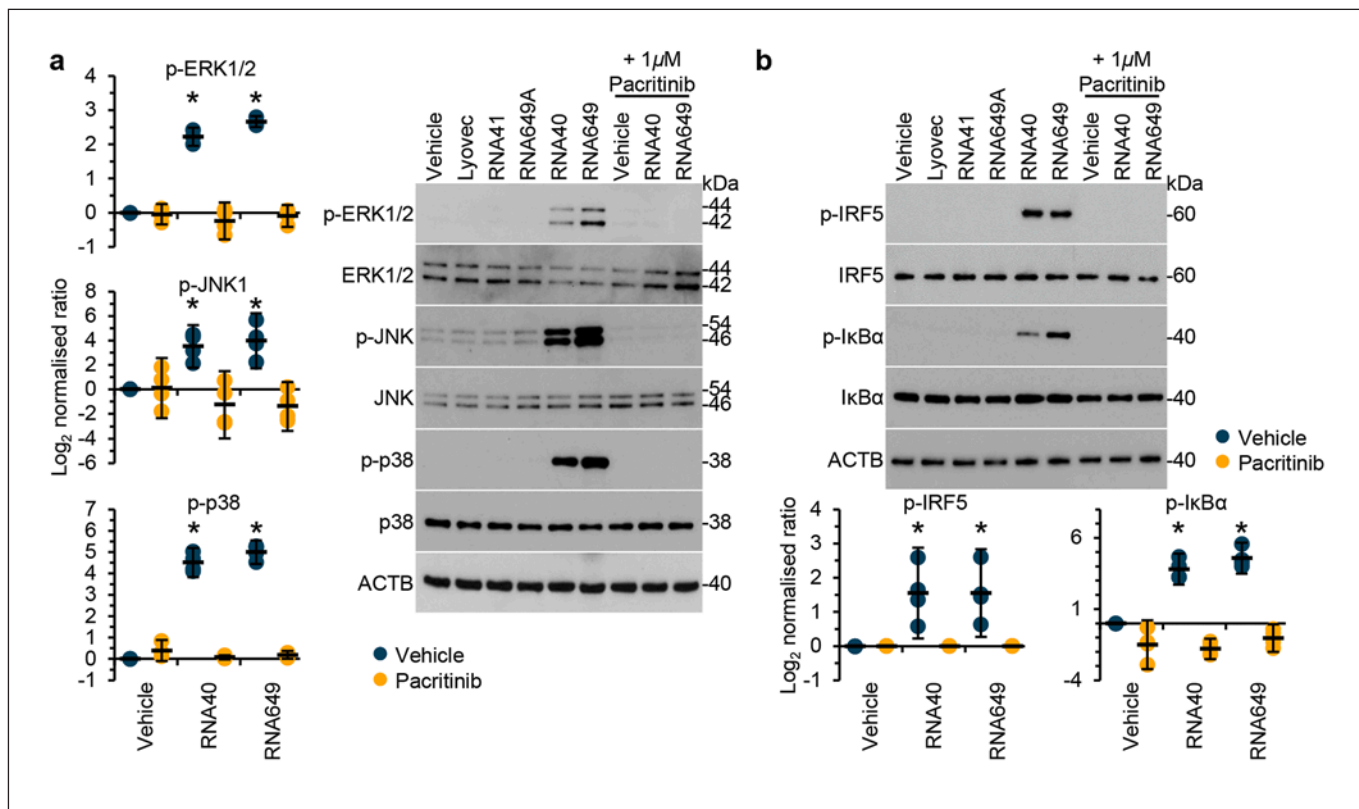


**Fig. 5.** Pacritinib inhibits downstream TLR8-mediated MAP kinase and NF- $\kappa$ B activation. Macrophages were pretreated with pacritinib or controls for 2 h and then treated for 6 h with 5  $\mu$ g mL<sup>-1</sup> GU-rich ssRNA.  $n = 4$ . **a** *Right*, representative western blots of ERK1/2, JNK, p38, and their phosphorylated forms. *Left*, densitometric analysis of blots. **b** *Top*, representative western blots of Ser<sup>32</sup>-phosphorylated I $\kappa$ B $\alpha$ , I $\kappa$ B $\alpha$ , Ser<sup>462</sup>-phosphorylated IRF5, and total IRF5 and ACTB. *Bottom*, densitometric analysis of blots.

#### Pacritinib Inhibits the Recruitment of the TAK1 Complex to IRAK1

As the recruitment of IRAK1 to the TLR8 myddosome results in the extensive ubiquitination and phosphorylation of IRAK1, we examined whether pacritinib inhibits these modifications. Treatment of macrophages with pacritinib indeed inhibited the TLR8-mediated phosphorylation and ubiquitination of IRAK1 (shown in Fig. 4). Since pacritinib inhibited the post-translational modifications of IRAK1, and these modifications are required for the recruitment of TRAF6 to IRAK1, as well as for TAB2 and TAB3 recruitment to the IRAK1-TRAF6 complex that triggers the association of TAK1 with the IRAK1-TRAF6 complex, we examined whether pacritinib inhibits this complex formation using co-immunoprecipitation. While TAK1, TAB2, and TRAF6 all co-immunoprecipitated with IRAK1 in RNA40 and RNA649-treated macrophages, pacritinib ablated this association (shown in Fig. 4).

The recruitment of TAK1 by TAB2 and TAB3 results in TAK1 activation, allowing the phosphorylation and activation of the downstream MAP kinase kinase (MKK) 4 and MKK7 that phosphorylate and activate MAPK8 and MAPK9 (also known as JNK1 and JNK2). Moreover, the binding of M1Ub chains to IRAK1 and their interaction with NEMO induces a conformational change that permits the phosphorylation and activation of IKK $\beta$  by TAK1. IKK $\beta$  then activates the Tpl2 kinase complex, which activates MEK1 and MEK2, the protein kinases that activate ERK1 and ERK2, and phosphorylates MKK3 and MKK6, which redundantly operate with MKK4 to phosphorylate and activate p38 $\alpha$  (MAPK14). Therefore, we evaluated whether pacritinib inhibited the TLR8-mediated MAP kinase activation cascade. At the concentration tested, pacritinib ablated the phosphorylation of ERK1, ERK2, JNK1, JNK2, and MAPK14 (shown in Fig. 5a). IKK $\beta$  also activates two of the principal transcription factors required for inflammatory cytokine pro-

duction. IKK $\beta$  activates NF- $\kappa$ B by phosphorylating its inhibitory components (I $\kappa$ B), leading to the release and nuclear translocation of NF- $\kappa$ B to initiate transcription [55], and it Ser<sup>462</sup>-phosphorylates and activates the transcription factor IFN regulatory factor 5 (IRF5) [56]. Similar to the MAP kinases, pacritinib inhibited the downstream activation of these kinases and transcription factors (shown in Fig. 5b).

## Discussion

Despite the development and widespread implementation of SARS-CoV-2 vaccines, COVID-19 continues to place a burden on healthcare systems throughout the world due to breakthrough infections, the unvaccinated, and long-haul COVID-19 survivors. Although most SARS-CoV-2 infections are asymptomatic or develop only mild or moderate symptoms, a fraction of infections can progress to CRS which can lead to acute respiratory distress syndrome with a case fatality rate of 5–8%, rising to ~15% in unvaccinated individuals >80 years [14–18]. Once CRS is initiated, antiviral therapy provides little benefit, and anti-inflammatory and immunosuppressive therapies are indicated. To date, a wide variety of anti-inflammatory drugs have been evaluated for their ability to suppress inflammation and the excessive pro-inflammatory immune responses during COVID-19 [57] with dexamethasone, baricitinib, tofacitinib, tocilizumab, and sarilumab among the drugs recommended for management of hospitalised adults [58]. Similarly, directly targeting the pro-inflammatory response is increasingly being considered as a treatment strategy for PLWH [59]. Although ART-mediated HIV-1 suppression has led to a significant reduction in the case fatality rate of HIV-1 infection and increases life expectancy, PLWH still have increased rates of morbidity and mortality compared with the general population. Chronic inflammation and hyperimmune activation persists even during ART-treated HIV-1 infection, and levels of inflammatory biomarkers including high circulating levels of IL-1 $\beta$ , IL-6, and TNF are predictive of risk for comorbidities as well as mortality [60, 61]. Thus, the suppression of inflammation and an excessive pro-inflammatory immune response is of potential therapeutic benefit.

There is emerging evidence for NLRP3 involvement in both HIV-1 pathogenesis [62–64] and in severe COVID-19 disease progression [65, 66]. As an integral and key component in the regulation of both TLR-mediated NLRP3 inflammasome activation [40] and the myddosome, IRAK1 is therefore involved in multiple IL-1- and

TLR-mediated signalling pathways that regulate immunity and inflammation. Thus, it is not surprising that dysregulation of these pathways is involved in a number of inflammatory diseases including autoimmune diseases, fibrotic diseases, and sepsis as well as in the initiation and promotion of multiple solid tumour and haematologic malignancies. As such, the pharmacologic inhibition of IRAK1 has potential therapeutic applications. Pacritinib markedly reduced secreted levels of the pro-inflammatory cytokines IL-17A, IL-2, and IL-6 [67] and suppressed and induced immunoglobulin synthesis in patients with myelofibrosis [68]. Pacritinib also inhibits constitutively activated IRAK1 phosphorylation in acute myeloid leukaemia cells [69] and breast cancer cells with duplication of 1q23.1 [70]. Here, we report that pacritinib effectively inhibits the TLR8-mediated pro-inflammatory cytokine responses to SARS-CoV-2 and HIV-1 RNA in the absence of active virus infection. This is of particular interest as increasing evidence has evolved demonstrating that SARS-CoV-2 ssRNA can be present long after acute infection [71, 72]. Thus, the impact of the continued presence of viral RNA on the persistent inflammatory response in long COVID-19 is of considerable interest.

Although the inhibition of IRAK1, a key mediator of the pro-inflammatory response raises concerns regarding immunosuppression and secondary infections; early clinical trials of pacritinib for autoimmune diseases, fibrotic diseases, and oncologic diseases have shown promising results with acceptable safety [73], and pacritinib has been FDA-approved in the USA for intermediate or high-risk primary or secondary myelofibrosis. Treatment regimens of pacritinib in COVID-19 patients and PLWH would be shorter than those for other targeted immunologic diseases and cancer, making it a safe therapeutic option. Pacritinib also inhibits JAK2, resulting in the suppression of Th1 cells that initiate CRS pathogenesis via CSF2 [74] and the reactivation of latent HIV-1 transcription [75].

The major limitation of the research presented is that we did not study the activation of TLR8 during active viral infection in vivo. However, activation of TLR8 does not require active infection [76], and the findings that pacritinib inhibits pro-inflammatory cytokine release in the absence of live infection is relevant in the context of persistent inflammation in PLWH despite ART-mediated viral suppression and also during long COVID-19. Future studies should address the effect and role of TLR8 signalling and IRAK1 inhibition during active infections and in long COVID-19.

In summary, our data demonstrate that pacritinib inhibits the SARS-CoV-2 and HIV-1 GU-rich ssRNA-in-



duced rapid activation, phosphorylation, and ubiquitination of IRAK1, leading to the inhibition of IL-6, TNF, and IL-1 $\beta$  release from human primary macrophages that does not require active viral infection. These data suggest that IRAK1 may prove to be an excellent therapeutic target to ameliorate SARS-CoV-2- and HIV-1-associated chronic inflammation.

### Statement of Ethics

Venous blood was drawn from HIV-seronegative healthy volunteers (aged between 18 and 65 years) at the San Diego Blood Bank or at UC San Diego Health Sciences using a protocol that was reviewed and approved by the Human Research Protections Program of the University of California, San Diego, in accordance with the requirements of the Code of Federal Regulations on the Protection of Human Subjects (45 CFR 46 and 21 CFR 50 and 56) and were fully compliant with the principles expressed in the Declaration of Helsinki, approval number #180485AW. All volunteers gave written informed consent prior to their participation, all samples were de-identified, and the donors remain anonymous.

### Conflict of Interest Statement

The authors have no conflicts of interest to declare.

### Funding Sources

This work was supported by the National Institute of Mental Health of the National Institutes of Health (NIH) (R01MH128021 to Grant R. Campbell), by the National Institute of Neurological

Disorders and Stroke of the NIH (R01NS104015 to Stephen A. Spector), and by the International Maternal Pediatric Adolescent AIDS Clinical Trials Network ([impaactnetwork.org](http://impaactnetwork.org)). Overall support for the International Maternal Pediatric Adolescent AIDS Clinical Trials (IMPAACT) Network is provided by the National Institute of Allergy and Infectious Diseases (NIAID) of the NIH under award numbers UM1AI068632 (IMPAACT LOC), UM1AI068616 (IMPAACT SDMC), and UM1AI106716 (IMPAACT LC), with co-funding from the Eunice Kennedy Shriver National Institute of Child Health and Human Development (NICHD) and the National Institute of Mental Health (NIMH). The content is solely the responsibility of the authors and does not necessarily represent the official views of the NIH.

### Author Contributions

Grant R. Campbell, Pratima Rawat, and Stephen A. Spector conceived, planned, and oversaw the studies. Grant R. Campbell and Pratima Rawat performed laboratory experiments. Grant R. Campbell, Pratima Rawat, and Stephen A. Spector performed data analysis, interpreted the data, and agreed to the final version submitted. Grant R. Campbell wrote the manuscript. Stephen A. Spector reviewed and edited the manuscript.

### Data Availability Statement

This study did not generate new unique reagents. This study did not generate/analyse datasets/code. Further information and requests for resources and reagents should be directed to and will be fulfilled by Grant R. Campbell ([gcampbell@health.ucsd.edu](mailto:gcampbell@health.ucsd.edu)).

### References

- Schulte-Schrepping J, Reusch N, Paclik D, Baßler K, Schlickeiser S, Zhang B, et al. Severe COVID-19 is marked by a dysregulated myeloid cell compartment. *Cell*. 2020;182(6):1419–40.e23.
- Reyes M, Filbin MR, Bhattacharyya RP, Sonny A, Mehta A, Billman K, et al. Plasma from patients with bacterial sepsis or severe COVID-19 induces suppressive myeloid cell production from hematopoietic progenitors in vitro. *Sci Transl Med*. 2021;13(598):eabe9599.
- Hadjadj J, Yatim N, Barnabei L, Corneau A, Boussier J, Smith N, et al. Impaired type I interferon activity and inflammatory responses in severe COVID-19 patients. *Science*. 2020;369(6504):718–24.
- Blanco-Melo D, Nilsson-Payant BE, Liu WC, Uhl S, Hoagland D, Möller R, et al. Imbalanced host response to SARS-CoV-2 drives development of COVID-19. *Cell*. 2020;181(5):1036–45.e9.
- Galani IE, Rovina N, Lampropoulou V, Triantafyllia V, Manioudaki M, Pavlos E, et al. Untuned antiviral immunity in COVID-19 revealed by temporal type I/III interferon patterns and flu comparison. *Nat Immunol*. 2021;22(1):32–40.
- Zheng M, Gao Y, Wang G, Song G, Liu S, Sun D, et al. Functional exhaustion of antiviral lymphocytes in COVID-19 patients. *Cell Mol Immunol*. 2020;17(5):533–5.
- Meckiff BJ, Ramírez-Suástegui C, Fajardo V, Chee SJ, Kusnadi A, Simon H, et al. Imbalance of regulatory and cytotoxic SARS-CoV-2-reactive CD4+ T cells in COVID-19. *Cell*. 2020;183(5):1340–53.e16.
- Kusnadi A, Ramírez-Suástegui C, Fajardo V, Chee SJ, Meckiff BJ, Simon H, et al. Severely ill COVID-19 patients display impaired exhaustion features in SARS-CoV-2-reactive CD8+ T cells. *Sci Immunol*. 2021;6(55):eabe4782.
- Galván-Peña S, Leon J, Chowdhary K, Michelson DA, Vijaykumar B, Yang L, et al. Profound Treg perturbations correlate with COVID-19 severity. *Proc Natl Acad Sci U S A*. 2021;118(37):e2111315118.
- Wang EY, Mao T, Klein J, Dai Y, Huck JD, Jaycox JR, et al. Diverse functional autoantibodies in patients with COVID-19. *Nature*. 2021;595(7866):283–8.
- Pedersen SF, Ho YC. SARS-CoV-2: a storm is raging. *J Clin Invest*. 2020;130(5):2202–5.
- Arunachalam PS, Wimmers F, Mok CKP, Perera R, Scott M, Hagan T, et al. Systems biological assessment of immunity to mild versus severe COVID-19 infection in humans. *Science*. 2020;369(6508):1210–20.
- McElvaney OJ, McEvoy NL, McElvaney OF, Carroll TP, Murphy MP, Dunlea DM, et al. Characterization of the inflammatory response to severe COVID-19 illness. *Am J Respir Crit Care Med*. 2020;202(6):812–21.

- 14 Huang C, Wang Y, Li X, Ren L, Zhao J, Hu Y, et al. Clinical features of patients infected with 2019 novel coronavirus in Wuhan, China. *Lancet*. 2020;395(10223):497–506.
- 15 Nanda A, Vura N, Gravenstein S. COVID-19 in older adults. *Aging Clin Exp Res*. 2020; 32(7):1199–202.
- 16 Bordallo B, Bellas M, Cortez AF, Vieira M, Pinheiro M. Severe COVID-19: what have we learned with the immunopathogenesis? *Adv Rheumatol*. 2020;60(1):50.
- 17 Zhu J, Ji P, Pang J, Zhong Z, Li H, He C, et al. Clinical characteristics of 3062 COVID-19 patients: a meta-analysis. *J Med Virol*. 2020; 92(10):1902–14.
- 18 Carsetti R, Zaffina S, Piano Mortari E, Terreri S, Corrente F, Capponi C, et al. Different innate and adaptive immune responses to SARS-CoV-2 infection of asymptomatic, mild, and severe cases. *Front Immunol*. 2020; 11:610300.
- 19 Antiretroviral Therapy Cohort Collaboration. Life expectancy of individuals on combination antiretroviral therapy in high-income countries: a collaborative analysis of 14 cohort studies. *Lancet*. 2008;372(9635):293–9.
- 20 Catalfamo M, Le Saout C, Lane HC. The role of cytokines in the pathogenesis and treatment of HIV infection. *Cytokine Growth Factor Rev*. 2012;23(4–5):207–14.
- 21 Heil F, Hemmi H, Hochrein H, Ampenberger F, Kirschning C, Akira S, et al. Species-specific recognition of single-stranded RNA via toll-like receptor 7 and 8. *Science*. 2004; 303(5663):1526–9.
- 22 Flannery S, Bowie AG. The interleukin-1 receptor-associated kinases: critical regulators of innate immune signalling. *Biochem Pharmacol*. 2010;80(12):1981–91.
- 23 Lee HK, Lund JM, Ramanathan B, Mizushima N, Iwasaki A. Autophagy-dependent viral recognition by plasmacytoid dendritic cells. *Science*. 2007;315(5817):1398–401.
- 24 Cervantes JL, La Vake CJ, Weinerman B, Luu S, O'Connell C, Verardi PH, et al. Human TLR8 is activated upon recognition of *Borrelia burgdorferi* RNA in the phagosome of human monocytes. *J Leukoc Biol*. 2013;94(6): 1231–41.
- 25 Greulich W, Wagner M, Gaidt MM, Stafford C, Cheng Y, Linder A, et al. TLR8 is a sensor of RNase T2 degradation products. *Cell*. 2019; 179(6):1264–75.e13.
- 26 Campbell GR, To RK, Hanna J, Spector SA. SARS-CoV-2, SARS-CoV-1, and HIV-1 derived ssRNA sequences activate the NLRP3 inflammasome in human macrophages through a non-classical pathway. *iScience*. 2021;24(4):102295.
- 27 Salvi V, Nguyen HO, Sozio F, Schioppa T, Gaudenzi C, Laffranchi M, et al. SARS-CoV-2-associated ssRNAs activate inflammation and immunity via TLR7/8. *JCI Insight*. 2021; 6(18):e150542.
- 28 Cushing L, Stochaj W, Siegel M, Czerwinski R, Dower K, Wright Q, et al. Interleukin 1/ Toll-like receptor-induced autophosphorylation activates interleukin 1 receptor-associated kinase 4 and controls cytokine induction in a cell type-specific manner. *J Biol Chem*. 2014; 289(15):10865–75.
- 29 Ferrao R, Zhou H, Shan Y, Liu Q, Li Q, Shaw DE, et al. IRAK4 dimerization and trans-autophosphorylation are induced by myddosome assembly. *Mol Cell*. 2014;55(6):891–903.
- 30 Vollmer S, Strickson S, Zhang T, Gray N, Lee KL, Rao VR, et al. The mechanism of activation of IRAK1 and IRAK4 by interleukin-1 and Toll-like receptor agonists. *Biochem J*. 2017;474(12):2027–38.
- 31 Lin SC, Lo YC, Wu H. Helical assembly in the MyD88-IRAK4-IRAK2 complex in TLR/IL-1R signalling. *Nature*. 2010;465(7300):885–90.
- 32 Brikos C, Wait R, Begum S, O'Neill LA, Saklatvala J. Mass spectrometric analysis of the endogenous type I interleukin-1 (IL-1) receptor signaling complex formed after IL-1 binding identifies IL-1RACp, MyD88, and IRAK-4 as the stable components. *Mol Cell Proteomics*. 2007;6(9):1551–9.
- 33 Motshwene PG, Moncrieffe MC, Grossmann JG, Kao C, Ayaluru M, Sandercock AM, et al. An oligomeric signaling platform formed by the Toll-like receptor signal transducers MyD88 and IRAK-4. *J Biol Chem*. 2009; 284(37):25404–11.
- 34 Jiang Z, Johnson HJ, Nie H, Qin J, Bird TA, Li X. Pellino 1 is required for interleukin-1 (IL-1)-mediated signaling through its interaction with the IL-1 receptor-associated kinase 4 (IRAK4)-IRAK-tumor necrosis factor receptor-associated factor 6 (TRAF6) complex. *J Biol Chem*. 2003;278(13):10952–6.
- 35 Cui W, Xiao N, Xiao H, Zhou H, Yu M, Gu J, et al.  $\beta$ -TrCP-mediated IRAK1 degradation releases TAK1-TRAF6 from the membrane to the cytosol for TAK1-dependent NF- $\kappa$ B activation. *Mol Cell Biol*. 2012;32(19):3990–4000.
- 36 Emmerich CH, Ordureau A, Strickson S, Arthur JS, Pedrioli PG, Komander D, et al. Activation of the canonical IKK complex by K63/M1-linked hybrid ubiquitin chains. *Proc Natl Acad Sci U S A*. 2013;110(38):15247–52.
- 37 Akira S, Uematsu S, Takeuchi O. Pathogen recognition and innate immunity. *Cell*. 2006; 124(4):783–801.
- 38 Ghosh TK, Mickelson DJ, Fink J, Solberg JC, Inglefield JR, Hook D, et al. Toll-like receptor (TLR) 2-9 agonists-induced cytokines and chemokines: I. Comparison with T cell receptor-induced responses. *Cell Immunol*. 2006; 243(1):48–57.
- 39 Vierbuchen T, Bang C, Rosigkeit H, Schmitz RA, Heine H. The human-associated archaeon *Methanospaera stadmanae* is recognized through its RNA and induces TLR8-dependent NLRP3 inflammasome activation. *Front Immunol*. 2017;8:1535.
- 40 Lin KM, Hu W, Troutman TD, Jennings M, Brewer T, Li X, et al. IRAK-1 bypasses priming and directly links TLRs to rapid NLRP3 inflammasome activation. *Proc Natl Acad Sci U S A*. 2014;111(2):775–80.
- 41 Wang Z, Wesche H, Stevens T, Walker N, Yeh WC. IRAK-4 inhibitors for inflammation. *Curr Top Med Chem*. 2009;9(8):724–37.
- 42 Cushing L, Winkler A, Jelinsky SA, Lee K, Korver W, Hawtin R, et al. IRAK4 kinase activity controls Toll-like receptor-induced inflammation through the transcription factor IRF5 in primary human monocytes. *J Biol Chem*. 2017;292(45):18689–98.
- 43 Singer JW, Fleischman A, Al-Fayoumi S, Mascarenhas JO, Yu Q, Agarwal A. Inhibition of interleukin-1 receptor-associated kinase 1 (IRAK1) as a therapeutic strategy. *Oncotarget*. 2018;9(70):33416–39.
- 44 William AD, Lee AC, Blanchard S, Poulsen A, Teo EL, Nagaraj H, et al. Discovery of the macrocycle 11-(2-pyrrolidin-1-yl-ethoxy)-14,19-dioxo-5,7,26-triaza-tetracyclo[19.3.1.1(2,6).1(8,12)]heptacosal(25),2(26),3,5,8,10,12(27),16,21,23-decaene (SB1518), a potent Janus kinase 2/fms-like tyrosine kinase-3 (JAK2/FLT3) inhibitor for the treatment of myelofibrosis and lymphoma. *J Med Chem*. 2011;54(213):4638–58.
- 45 Campbell GR, To RK, Spector SA. TREM-1 protects HIV-1-infected macrophages from apoptosis through maintenance of mitochondrial function. *mBio*. 2019;10(6):e02638–19.
- 46 Campbell GR, Bruckman RS, Chu YL, Trout RN, Spector SA. SMAC mimetics induce autophagy-dependent apoptosis of HIV-1-infected resting memory CD4+ T cells. *Cell Host Microbe*. 2018;24(15):689–e7.
- 47 Campbell GR, To RK, Zhang G, Spector SA. SMAC mimetics induce autophagy-dependent apoptosis of HIV-1-infected macrophages. *Cell Death Dis*. 2020;11:590.
- 48 Schindelin J, Arganda-Carreras I, Frise E, Kaynig V, Longair M, Pietzsch T, et al. Fiji: an open-source platform for biological-image analysis. *Nat Methods*. 2012;9(7):676–82.
- 49 Bergemann TL, Wilson J. Proportion statistics to detect differentially expressed genes: a comparison with log-ratio statistics. *BMC Bioinformatics*. 2011;12:228.
- 50 Yamin TT, Miller DK. The interleukin-1 receptor-associated kinase is degraded by proteasomes following its phosphorylation. *J Biol Chem*. 1997;272(34):21540–7.
- 51 Pauls E, Nanda SK, Smith H, Toth R, Arthur JSC, Cohen P. Two phases of inflammatory mediator production defined by the study of IRAK2 and IRAK1 knock-in mice. *J Immunol*. 2013;191(5):2717–30.
- 52 Moen SH, Ehrnström B, Kojen JF, Yurchenko M, Beckwith KS, Afset JE, et al. Human toll-like receptor 8 (TLR8) is an important sensor of pyogenic bacteria, and is attenuated by cell surface TLR signaling. *Front Immunol*. 2019; 10:1209.
- 53 Gaidt MM, Ebert TS, Chauhan D, Schmidt T, Schmid-Burgk JL, Rapino F, et al. Human monocytes engage an alternative inflammasome pathway. *Immunity*. 2016;44(4):833–46.

- 54 Costa-Junior HM, Sarmiento Vieira F, Coutinho-Silva R. C terminus of the P2X7 receptor: treasure hunting. *Purinergic Signal*. 2011; 7(1):7–19.
- 55 Zhang J, Clark K, Lawrence T, Pegg MW, Cohen P. An unexpected twist to the activation of IKK $\beta$ : TAK1 primes IKK $\beta$  for activation by autophosphorylation. *Biochem J*. 2014;461(3):531–7.
- 56 Lopez-Pelaez M, Lamont DJ, Pegg M, Shpiro N, Gray NS, Cohen P. Protein kinase IKK $\beta$ -catalyzed phosphorylation of IRF5 at Ser462 induces its dimerization and nuclear translocation in myeloid cells. *Proc Natl Acad Sci U S A*. 2014;111(49):17432–7.
- 57 Kawazoe M, Kihara M, Nanki T. Antirheumatic drugs against COVID-19 from the perspective of rheumatologists. *Pharmaceuticals*. 2021;14(12):1256.
- 58 COVID-19 Treatment Guidelines Panel. *National Institutes of Health [Internet]*. Bethesda, Maryland, USA: Coronavirus disease 2019 (COVID-19) treatment guidelines; 2019 [cited 23 May 2022]. Available from: <https://www.covid19treatmentguidelines.nih.gov/>.
- 59 Kettelhut A, Bowman E, Funderburg NT. Immunomodulatory and anti-inflammatory strategies to reduce comorbidity risk in people with HIV. *Curr HIV/AIDS Rep*. 2020; 17(4):394–404.
- 60 Utay NS, Hunt PW. Role of immune activation in progression to AIDS. *Curr Opin HIV AIDS*. 2016;11(2):131–7.
- 61 Tenorio AR, Zheng Y, Bosch RJ, Krishnan S, Rodriguez B, Hunt PW, et al. Soluble markers of inflammation and coagulation but not T-cell activation predict non-AIDS-defining morbid events during suppressive antiretroviral treatment. *J Infect Dis*. 2014;210(8): 1248–59.
- 62 Zhang Q, Fan HW, Zhang JZ, Wang YM, Xing HJ. NLRP3 rs35829419 polymorphism is associated with increased susceptibility to multiple diseases in humans. *Genet Mol Res*. 2015;14(4):13968–80.
- 63 Feria MG, Taborda NA, Hernandez JC, Rugeles MT. HIV replication is associated to inflammasomes activation, IL-1 $\beta$ , IL-18 and caspase-1 expression in GALT and peripheral blood. *PLoS One*. 2018;13(4):e0192845.
- 64 Kearns AC, Liu F, Dai S, Robinson JA, Kiernan E, Tesfaye Cheru L, et al. Caspase-1 activation is related with HIV-associated atherosclerosis in an HIV transgenic mouse model and HIV patient cohort. *Arterioscler Thromb Vasc Biol*. 2019;39(9):1762–75.
- 65 Toldo S, Bussani R, Nuzzi V, Bonaventura A, Mauro AG, Cannatà A, et al. Inflammasome formation in the lungs of patients with fatal COVID-19. *Inflamm Res*. 2021;70(1):7–10.
- 66 Rodrigues TS, de Sá KSG, Ishimoto AY, Becerra A, Oliveira S, Almeida L, et al. Inflammasomes are activated in response to SARS-CoV-2 infection and are associated with COVID-19 severity in patients. *J Exp Med*. 2021; 218(3):e20201707.
- 67 Singer JW, Al-Fayoumi S, Taylor J, Velichko S, O'Mahony A. Comparative phenotypic profiling of the JAK2 inhibitors ruxolitinib, fedratinib, momelotinib, and pacritinib reveals distinct mechanistic signatures. *PLoS One*. 2019;14(9):e0222944.
- 68 Mascarenhas J, Hoffman R, Talpaz M, Gerds AT, Stein B, Gupta V, et al. Pacritinib vs best available therapy, including ruxolitinib, in patients with myelofibrosis: a randomized clinical trial. *JAMA Oncol*. 2018;4(5):652–9.
- 69 Hosseini MM, Kurtz SE, Abdelhamed S, Mahmood S, Davare MA, Kaempf A, et al. Inhibition of interleukin-1 receptor-associated kinase-1 is a therapeutic strategy for acute myeloid leukemia subtypes. *Leukemia*. 2018; 32(11):2374–87.
- 70 Goh JY, Feng M, Wang W, Oguz G, Yatim S, Lee PL, et al. Chromosome 1q21.3 amplification is a trackable biomarker and actionable target for breast cancer recurrence. *Nat Med*. 2017;23(11):1319–30.
- 71 Tiwari L, Gupta P, Singh CM, Singh PK. Persistent positivity of SARS-CoV-2 nucleic acid in asymptomatic healthcare worker: infective virion or inactive nucleic acid? *BMJ Case Rep*. 2021; 14(3): e241087. <http://dx.doi.org/10.1136/bcr-2020-241087>.
- 72 Walsh KA, Jordan K, Clyne B, Rohde D, Drummond L, Byrne P, et al. SARS-CoV-2 detection, viral load and infectivity over the course of an infection. *J Infect*. 2020;81(3): 357–371. <http://dx.doi.org/10.1016/j.jinf.2020.06.067>.
- 73 Singer JW, Al-Fayoumi S, Ma H, Komrokji RS, Mesa R, Verstovsek S. Comprehensive kinase profile of pacritinib, a nonmyelosuppressive Janus kinase 2 inhibitor. *J Exp Pharmacol*. 2016;8:11–9.
- 74 Betts BC, Bastian D, Iamsawit S, Nguyen H, Heinrichs JL, Wu Y, et al. Targeting JAK2 reduces GVHD and xenograft rejection through regulation of T cell differentiation. *Proc Natl Acad Sci U S A*. 2018;115(7):1582–7.
- 75 Gavegnano C, Detorio M, Montero C, Bosque A, Planelles V, Schinazi RF. Ruxolitinib and tofacitinib are potent and selective inhibitors of HIV-1 replication and virus reactivation in vitro. *Antimicrob Agents Chemother*. 2014; 58(4):1977–86.
- 76 Campbell GR, Rawat P, Bruckman RS, Spector SA. Human immunodeficiency virus type 1 Nef inhibits autophagy through transcription factor EB sequestration. *PLoS Pathog*. 2015;11(6):e1005018.